

Occluded Person Re-Identification with Deep Learning: A Survey and Perspectives

Enhao Ning ^{a,1}, Changshuo Wang ^{a,b,1}, Huang Zhang^c, Xin Ning ^{a,*} and Prayag Tiwari ^{d,*}

^a*Institute of Semiconductors, Chinese Academy of Sciences, Beijing, 100083, China*

^b*Center of Materials Science and Optoelectronics Engineering & School of Microelectronics, University of Chinese Academy of Sciences, Beijing, 100083, China*

^c*School of Software, Xinjiang University, Xinjiang, 830000, China*

^d*School of Information Technology, Halmstad University, Halmstad, 30118, Sweden*

ARTICLE INFO

Keywords:

Occluded Person Re-identification
Literature Survey and Perspectives
Multimodal Person Re-identification
3D Person Re-identification.

ABSTRACT

Person re-identification (Re-ID) technology plays an increasingly crucial role in intelligent surveillance systems. Widespread occlusion significantly impacts the performance of person Re-ID. Occluded person Re-ID refers to a pedestrian matching method that deals with challenges such as pedestrian information loss, noise interference, and perspective misalignment. It has garnered extensive attention from researchers. Over the past few years, several occlusion-solving person Re-ID methods have been proposed, tackling various sub-problems arising from occlusion. However, there is a lack of comprehensive studies that compare, summarize, and evaluate the potential of occluded person Re-ID methods in detail. In this review, we start by providing a detailed overview of the datasets and evaluation scheme used for occluded person Re-ID. Next, we scientifically classify and analyze existing deep learning-based occluded person Re-ID methods from various perspectives, summarizing them concisely. Furthermore, we conduct a systematic comparison among these methods, identify the state-of-the-art approaches, and present an outlook on the future development of occluded person Re-ID.

1. Introduction

With the increasing integration and intelligence of surveillance equipment (Bedagkar-Gala & Shah, 2014) in recent years, person re-identification (Re-ID) technology has significantly advanced. This technology finds extensive application in sensitive and specialized domains, such as medicine, rescue operations, criminal investigations, and surveillance. These fields often operate in complex and dynamic environments. Consequently, the rapid and accurate localization and identification of specific targets in multi-camera occlusion scenarios hold immense practical significance.

Given the complexity and variability of real-life scenes, where people and objects move randomly, and surveillance devices typically cover wide areas, the likelihood of occluded individuals is high. Occlusion can have a severe impact on visual information, rendering the affected features unreliable. Occlusion can occur due to object interference, changes in pedestrian pose, clothing, and perspective. In early pedestrian representations, researchers primarily relied on basic, local visual attributes extracted from images, such as color, texture, edges, and corner points. These features capture geometric shapes and pixel distributions in images but are highly sensitive to external factors, lacking robustness and generalization. The development of deep

learning has introduced high-level visual features. Compared with low-level visual features, high-level features are more adaptive to occlusions, noises and pose changes, and have stronger robustness in complex environments. Consequently, numerous researchers have developed a multitude of methods to address the prevalent occlusion problem. In general, the occlusion problem is divided into three sub-problems: (1) Noise problem. The problem of interference by multiple and mixed information from the features in the acquisition of complex scenes. (2) Missing problem. The problem of incomplete pedestrian features is due to only a part of the pedestrian being captured. (3) Alignment problem. Owing to the change in posture, perspective, and position, the features cannot correspond one-to-one, which causes distraction, shared location misalignment, and other issues. The study of occlusion also involves the separation of humans and backgrounds to extract human features as the core. Methods to extract fine-grained, highly discriminative, and more essential features with reference and value have also been studied.

We want to identify the current state-of-the-art and limitations of existing methods and discover unexplored areas. Specifically, we present methods for dealing with occluded person Re-ID that were submitted in top international journals or conferences before 2023. We classify deep learning-based occluded person Re-ID according to the network structure of extracted features (CNN-based, transformer-based, and hybrid structure-based), the way features are extracted (uni-modal and multi-modal), and the hierarchical structure of features (2d and 3d). (see Figure 1). First, due to the powerful performance of convolutional neural networks (CNNs) in image matching tasks, CNN-based methods have

*Corresponding author.

E-mail addresses: ningenhao@163.com (E.N.),

wangchangshuo@semi.ac.cn (C.W.), zhjh1998@outlook.com (H. Zhang),

ningxin@semi.ac.cn (X.N.), prayag.tiwari@ieee.org (P.T.)

ORCID(s):

¹Equal contribution.

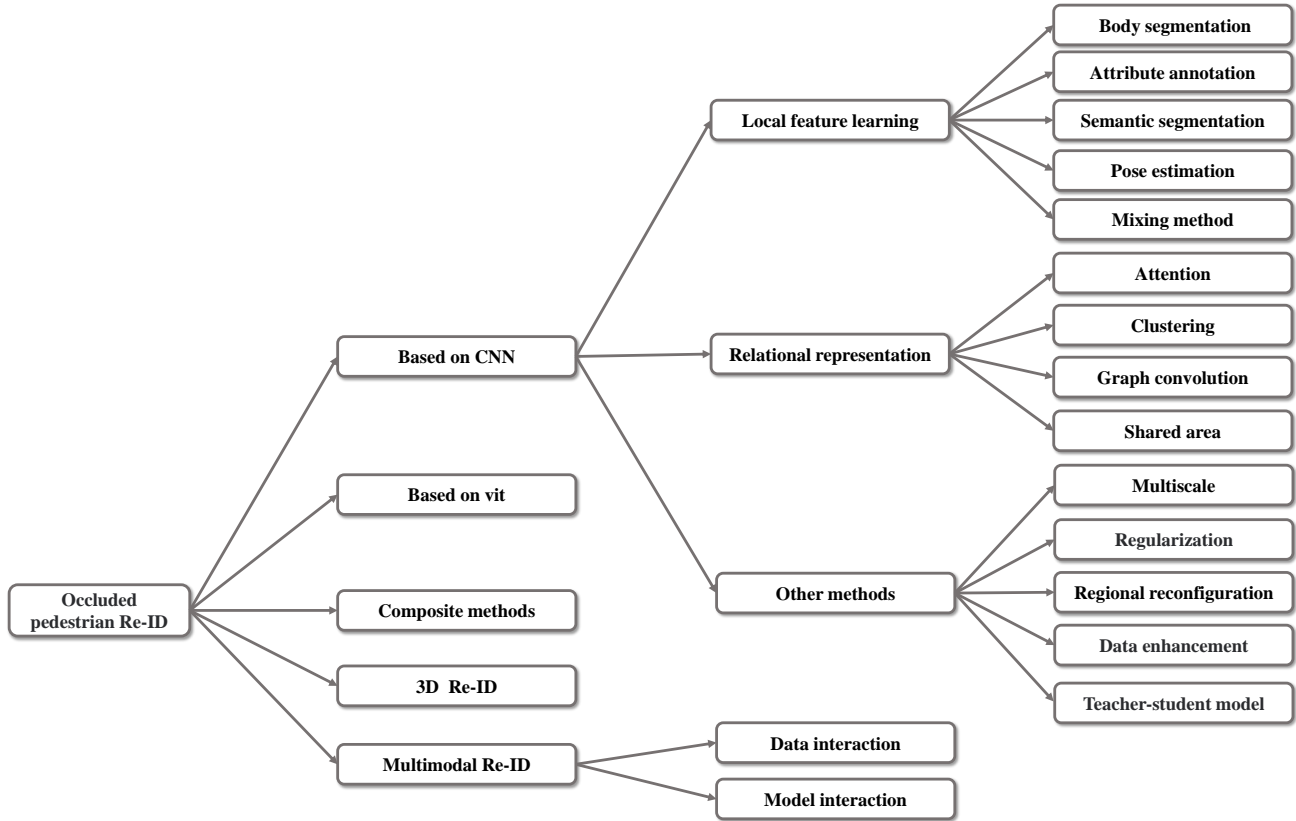


Figure 1: Overall structure of the survey.

become one of the mainstream methods to deal with occlusion problems in person Re-ID. Therefore, we treat the cnn-based methods as the first class of methods to deal with the occlusion problem. Secondly, based on the success of transformer in the field of natural language, in recent years, vit has also been widely used to deal with the occlusion problem in pedestrian re-identification with good results. Therefore, we treat transformer-based methods as the second category. The third class of methods are some composite methods. For example, the complementary nature of CNN and vit is exploited to form a hybrid structure. The fourth and fifth class of methods are based on 3D and multimodal to deal with the occlusion problem in person Re-ID. They deal with more scenarios and are a relatively novel approach.

In general, the contributions of this study are as follows:

1) This study focuses on addressing the occlusion problem in person Re-ID models, which is crucial for achieving high accuracy and robustness. We present a scientific and comprehensive review of past and current state-of-the-art approaches.

2) The current review of person Re-ID methods lacks sufficient coverage of approaches based on ViT. Given the excellent performance of ViT in occluded person Re-ID, we include a discussion of this method and its hybrid variants

in our study, offering researchers new ideas and options for addressing the occlusion problem.

3) We creatively incorporate 3D person Re-ID and multimodal person Re-ID, which have become popular in recent years. These novel methods can better solve the occlusion problem by utilizing additional depth or modal information, thus improving the performance and reliability of person Re-ID.

4) We anticipate advancements in occluded person Re-ID and firmly believe that continued research and innovation will lead to the development of more effective methods and technologies for addressing the occlusion problem. These advancements will inspire and drive progress in the field of person Re-ID.

2. Literature review

In the field of person Re-ID, there is a relative scarcity of specialized reviews compared to methodological articles. And they all focus on specific problems. These surveys are listed in Table 1. Bedagkar-Gala & Shah (2014) focuses on the challenges of person Re-ID and divides it into open-set Re-ID and closed-set Re-ID based on the fixity of the gallery. Zheng et al. (2016) divides the methods of person Re-ID into methods for images and methods for videos based on the matching strategy. Gou et al. (2018) provides a more detailed study of the features, metrics, and datasets of person Re-ID.

Table 1

The summary of person-reported surveys in recent years.

Survey	Venue
A survey of approaches and trends in person Re-ID (Bedagkar-Gala & Shah, 2014)	IVC2014
Person Re-ID Past, Present and Future (Zheng et al., 2016)	arXiv2016
A systematic evaluation and benchmark for person Re-ID: Features, metrics, and datasets (Gou et al., 2018)	TPAMI2019
Beyond intra-modality discrepancy: A comprehensive survey of heterogeneous person Re-ID (Wang et al., 2019b)	arXiv2019
A Survey of Open-World Person Reidentification (Leng et al., 2019)	TCSVT2020
Survey on Reliable Deep Learning-Based person Re-ID Models: Are We There Yet? (Lavi et al., 2020)	arXiv2020
Deep Learning for Person Reidentification: A Survey and Outlook (Ye et al., 2021b)	TPAMI2021
SSS-PR: A short survey of surveys in person Re-ID (Yaghoubi et al., 2021)	PRL2021
Deep learning-based person Re-ID methods: A survey and outlook of recent works (Ming et al., 2022)	IVC2022
Deep Learning-based Occluded person Re-ID: A Survey (Peng et al., 2022)	arXiv2022

Wang et al. (2019b) focuses on heterogeneous person Re-ID. According to the application scenario, it classifies the methods into four categories — low-resolution, infrared, sketch, and text. Leng et al. (2019) focuses on open-world Re-ID tasks. Lavi et al. (2020) classifies Re-ID into single feature learning based approaches and multi-feature learning based approaches based on feature learning strategies. Ye et al. (2021b) provides a more detailed explanation of Re-ID for open and closed settings, and introduces methods such as transmembrane states, unsupervised. Yaghoubi et al. (2021) provides a more multidimensional classification of the person Re-ID problem. Ming et al. (2022) classifies the methods of person Re-ID into four categories based on metric learning and representation learning, and adds the latest methods. Peng et al. (2022) focuses on image-based obscured person Re-ID methods. However, these investigations are inevitably affected by a number of inherent limitations. Considering the widespread existence of the occlusion problem in pedestrian recognition, research on occluded person Re-ID is essential. Therefore, we provide an in-depth summary and comprehensive analysis of methods and prospects in occluded person Re-ID to advance future developments.

3. Datasets and Evaluation Protocols

3.1. Datasets

Occluded person Re-ID datasets can be divided into two categories: partial person and occluded person Re-ID datasets. The pedestrian images of the occluded person Re-ID datasets have occlusion information interference and are not cropped. The pedestrian image portion of the partial person Re-ID dataset is present and artificially cropped. Examples of partial/occluded person Re-ID datasets are shown in Figure 2.

Occluded-DukeMTMC (Miao et al., 2019) was collected from DukeMTMC-reID (Zheng et al., 2017), containing 15,618 training images of 708 pedestrians, 2,210 query images of 519 pedestrians, and 17,661 gallery images of 1,110 pedestrians for testing. Of these images, 9% of the training set, 100% of the query set, and 10% of the gallery are occluded images. Obstacles include cars, bicycles, trees, and other pedestrians, adding complexity to the dataset.

P-ETHZ (Zheng et al., 2015b) is an image-based occluded person Re-ID dataset, modified by ETHZ (Ess et al., 2008). It has 3,897 images containing 85 pedestrian identities with 1 to 30 full-body and occluded pedestrian images per identity.

P-DukeMTMC-reID (Zhuo et al., 2018) was modified from DukeMTMC-reID (Zheng et al., 2017), containing a total of 24,143 images of 1,299 pedestrians, and each identity has a full-body and occlusion image; the pedestrian in the image is occluded by different objects, such as other pedestrians, cars, and signage.

Occluded-REID (Zheng et al., 2015b) has 2,000 images of 200 pedestrians, each pedestrian corresponding to 5 occlusion and 5 whole body images, collected from Sun Yat-sen University. The dataset includes different viewpoints and types of severe occlusion, which challenges person Re-ID.

Occluded-DukeMTMC-VideoReID (Hou et al., 2021) was reorganized from the DukeMTMC-VideoReID (Wu et al., 2018) dataset. The training set contains 1,702 trajectory segments covering 702 pedestrians, the test set queries cover 661 pedestrians, and the gallery covers 1,110. More than 70% of the videos are occluded, including different perspectives and a variety of obstacles, such as cars, trees, bicycles, and other pedestrians.

Partial-ReID (Zheng et al., 2015b) has 600 images of 60 pedestrians, 5 partial and 5 full-body images for each pedestrian. Using the visible parts, they are manually cropped to form new partial images. The images are collected from different perspectives, backgrounds and occlusions in a university campus.

Partial-iLIDS (He et al., 2018) was derived from iLIDS (Zheng et al., 2011) and contains 238 images of 119 pedestrians. Each pedestrian corresponds to one manually cropped non-occluded partial image and one full-body image. The partial image is used as a query, and the full-body image is used as a search library. It was shot by multiple non-overlapping cameras, mostly for test sets.

Partial-CAVIAR (He et al., 2018) was derived from CAVIAR (Cheng et al., 2011) and contains 142 images of 72 pedestrians. The partial map is generated by randomly picking half of the overall image of each pedestrian.

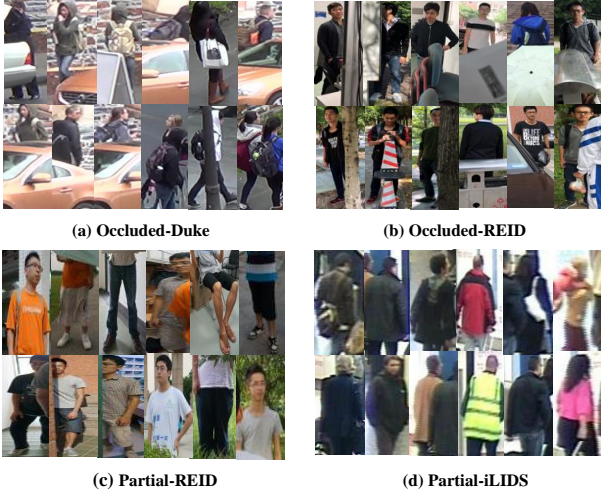


Figure 2: Examples of four commonly used occluded person Re-ID datasets.

P-CUHK03 (Kim & Yoo, 2017) was constructed based on CUHK03 (Li et al., 2014), with a total of 1,360 pedestrian images, wherein 15,080 images corresponding to 1,160 pedestrians are used as a training set, and the remaining 100 pedestrians are used as a validation and test set. Two of the images are selected to generate 10 local body query images with a spatial area ratio, and the remaining three images are used as whole body gallery images.

3.2. Evaluation Protocols

In the field of occluded person Re-ID, the commonly used evaluation metrics are Cumulative Matching Characteristic (CMC) curves and mean Average Precision (mAP).

CMC curves are based on the principle of ranking the similarity between the query image and the image library, and the higher the top image, the higher the similarity with the query image. Then, the top- k accuracy ACC^k of the query image is calculated based on this ranking. If the first k samples contain the query target, then ACC^k is 1, $k \in \{1, 2, 3, \dots\}$. Otherwise, ACC^k is 0. Finally, the ACC^k curves for all targets are summed and divided by the total number of targets to obtain CMC- k .

mAP better reflects the degree to which all correct target pictures are at the top of the sorted list. Compared with the CMC curve, it can more comprehensively measure the performance of Re-ID algorithms, where P is the precision rate, which refers to the proportion of correct samples among all samples. It reflects the accuracy of the correct samples in the output. The AP is the average of all correct samples predicted by the model. It reflects how well the model works on a single category and is the average of the accuracy of each correct prediction. Since there is more than one class in the recognition, the average AP value needs to be calculated for all classes, so the average accuracy of each class is added and divided by the total number of classes to obtain mAP.

The CMC curve cannot consider the hits of the samples with lower rankings, while mAP takes all samples into account. Therefore, they are important and complementary.

4. Deep Learning Methods

4.1. Based on CNN

Convolutional neural networks (CNNs) have emerged as one of the leading methods for learning pedestrian representations from RGB images. By using local perceptual fields and learning filters, CNNs can extract powerful features that capture regional information about local features of pedestrians. These features are then compressed and mapped to higher-level representations. Researchers have refined them to be usable for pedestrian matching tasks in complex realistic scenarios. We classify it into local feature learning, relational representation, mixing methods, and other methods.

4.1.1. Local Feature Learning

Local feature-learning performs better at handling regional features, and it has unique advantages for occlusion region recognition and location compared with global features. According to its implementation of different local feature methods, we divide them into human segmentation, pose estimation, human parsing, attribute annotation, and hybrid methods (see Figure 3).

Body Segmentation. By leveraging the characteristic of pedestrians walking upright, our method extracts improved local features through the segmentation of the original image or feature map. The segmentation results can take the form of stripes, fixed regions, or small patches (see Figure 4).

However, segmentation does not have the process of identifying occlusions, so it is sensitive to noise. CBDB-Net (Tan et al., 2021) evenly divides the strips on the feature map and discards each strip one by one to output multiple incomplete feature maps, which forces the model to learn a more robust pedestrian representation in an environment with incomplete information. The DPPR (Kim & Yoo, 2017) predefines thirteen bounding boxes for the whole-body image, including the whole image, half-body image, and horizontal part image, and extracts features from each part. At the same time, an attention-based matching mechanism is introduced to make the feature weight of the same body part larger, which can alleviate the information loss caused by occlusion. At the same time, an attention-based matching mechanism is introduced to make the feature weight of the same body part larger, which can alleviate the information loss caused by occlusion. OCNet (Kim et al., 2022) introduces a relationship-based approach to deal with occlusion problems. OCNet (Kim et al., 2022) divides the feature map horizontally into top and bottom features and takes 1/4 of the middle width as the central feature. Then, it is put into the relational adaptive module consisting of two shared layers together with the global feature map. The alignment problem between regional features is handled by relations, and weights are introduced to suppress noise interference.

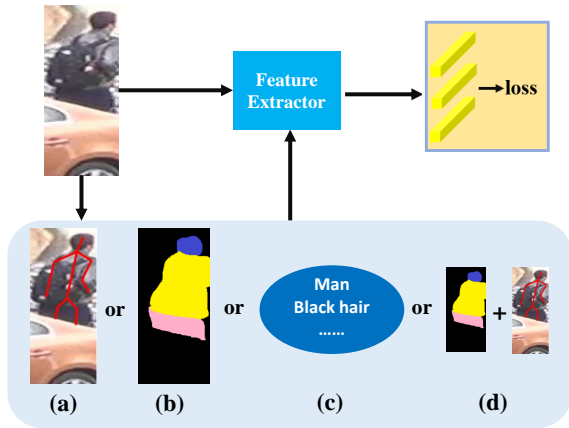


Figure 3: Four different local feature learning methods: (a) indicates pose estimation. (b) indicates semantic segmentation. (c) indicates attribute annotations. (d) indicates the mixing method.

Pose Estimation. Pose estimation extracts semantic information at the image pose level by exploiting the highly structured human skeleton. The interference of noise is suppressed in a guided or fused manner.

HOReID (Wang et al., 2020a) introduced a learnable relational matrix. The human body key points obtained from the pose estimation are regarded as nodes in the graph, and finally, a topology graph is formed to suppress noise interference. PMFB (Miao et al., 2021) uses pose estimation to obtain confidence and coordinates of human keypoints. Then, a threshold is set to filter the occluded regions. Finally, the visible part is used to constrain the feature response at channel level to solve the occlusion problem. PGMANet (Zhai et al., 2021) generates an attention mask using a human heat map. The interference of noise is removed jointly by the dot product of feature maps and guidance of higher-order relations.

Researchers generally use pose estimation in two directions: 1) to obtain semantic features through pose estimation, identify noise points, and better remove noise interference, and 2) to localize human regions through pose estimation and thus solve the problem of alignment and local feature extraction. AACN (Xu et al., 2018) uses pose points to locate pedestrian body regions and introduces a posture-guided visibility score to separate occlusions. DAReID (Xu et al., 2021) adopts a dual-branch structure, in which the mask branch extracts more discriminative local features based on the spatial attention module guided by pose estimation, and the global branch enhances the representation of human discriminative information through feature activation. DSAREID (Zhang et al., 2019) estimates dense semantic information at the 2D level by a pre-trained DensePose (Güler et al., 2018) model and maps a set of dense 3D semantic alignment components. Local features are extracted by integrating neighboring components. Finally, the global and local features are fused into the final feature. PGFL-KD (Zheng et al., 2021) takes the local features of the semantic layer

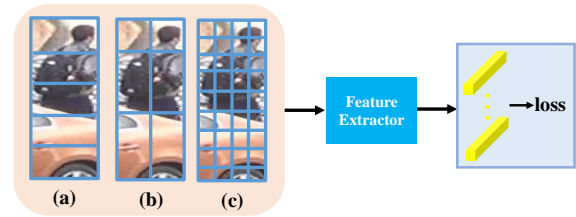


Figure 4: Three common Body Segmentation schematics: (a) indicates stripes. (b) indicates fixed areas. (c) indicates small blocks.

as queries and looks for more prominent foreground regions in the feature map to obtain enhanced foreground features. Based on this feature, interactive training and knowledge distillation are performed to constrain the learning of the backbone network. ACSAP (He et al., 2021c) uses pose keypoints to guide the adversarial generation network to remove noise interference by weakening the spatial relationship between the front and back blocks. PDC (Su et al., 2017) obtains 6 body regions according to 14 key points of pose, rotates and scales each part, and uses an improved PTN network to learn the parameters of affine transformation. These local features are automatically placed at certain locations in the drawing to resolve alignment issues. PVPM (Gao et al., 2020b) trains a visibility predictor based on the correspondence between visibility parts. After that, the alignment problem is solved by generating part pseudo-labels through graph matching.

Semantic Segmentation. By introducing a human parsing model, the interference of noise is identified and removed in the form of segmentation or semantic parsing.

SPReID (Kalayeh et al., 2018) generates probability maps associated with five different body regions based on the trained pedestrian class semantic parsing model Inception-V3 (Szegedy et al., 2016), namely, foreground, head, upper body, lower body, and shoes. Then, the probability map is fused with the semantic region features after bilinear interpolation to activate different parts and remove the interference of occlusion. CoAttention (Lin & Wang, 2021) takes the parsing mask of the local image of the pedestrian's body as a query and constructs a mapping while introducing a self-attentive mechanism to filter occlusions. MMGA (Cai et al., 2019) first separates pedestrians from images into upper and lower body using JPPNet (Liang et al., 2018). Then, two attention modules are designed; the first is used to filter the interference from the background, and the second generates the corresponding spatial and channel attentions to extract different features guided by the whole, upper, and lower body masks. Finally, element-level multiplication is performed as the final feature. HPNet (Huang et al., 2020) uses the COCO (Lin et al., 2014) dataset to train the human body parsing model to obtain labels for the four main body parts, based on which the parsing model and overall network are trained in a multitasking manner while generating visibility scores to remove occlusions.

Semantic segmentation-based approaches also contribute to enhancing the diversity of features. In the case of SORN

(Zhang et al., 2020), a three-branch model composed of a global branch, a local branch, and a semantic branch is designed. The global branch aims to obtain global features through normalization and feature aggregation. Meanwhile, the local branch leverages prior knowledge of the pedestrian body structure to generate pedestrian body parts and derive local features through mapping, pooling, and normalization. The semantic branch first uses the DANet (Fu et al., 2019) model to pre-train the semantic labels of the data, trains a semantic segmentation model on the DensePose-COCO dataset (Güler et al., 2018), introduces label smoothing to optimize the semantic labels, and forms a foreground pedestrian body region by aggregating the semantic segmentation part to realize the separation of background and pedestrians. SGSFA (Ren et al., 2020) introduces a semantic alignment branch and spatial feature alignment branch. The former achieves semantic alignment through element-level multiplication. The latter is based on regional spatial alignment achieved by body structure.

Attribute annotation. The occlusion problem is handled by introducing attribute annotation.

ASAN (Jin et al., 2021) extracts the visible part of human features by combining attribute information and weak supervision. Attribute information is a semantic level attribute annotation. Based on the visibility part determination, a region visibility matching algorithm is introduced to achieve the effect of denoising.

Mixing method. Introducing more than two kinds of external information can help the model remove the interference of noise in the form of feature interaction or co-guidance.

GASM (He & Liu, 2020) proposes an architecture for learning salient information, which separates pedestrians from background by using semantic information, removes occlusion interference by pose estimation, and then fuses the two features to guide model learning. SSPReID (Quispe & Pedrini, 2019) designs a joint learning method to combine salient and semantic features. Five different semantic features of the human body are obtained by human body parsing. The saliency features utilize the regions of highest attention in the graph. These features are fused with global features and finally concatenated together to form the final features. TSA (Gao et al., 2020a) introduces two kinds of area features for the pose change problem, one guided by pose keypoints and one guided by partial masks of the human parsing model, after which the two are fused. Using interaction can solve the pose change problem, while using pose and segmentation can also suppress noise and thus solve the occlusion problem. FGSA (Zhou et al., 2020a) proposes a pose resolution network for complex pose changes to deal with local locations and the relationships between them. Attribute interaction learning is designed for local feature information extraction corresponding to pose points, which is achieved by training an intermediate attribute classification model that treats attribute recognition as a multi-category labeling problem. Finally, a local enhanced alignment model is added in the feature fusion phase, that is, less weight is added to

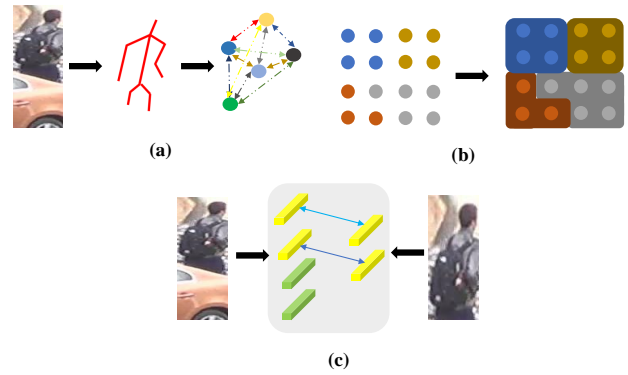


Figure 5: (a) Schematic diagram showing figure convolution. (b) Schematic representation of clustering. (c) Schematic representation of the shared area.

the background and more weight is added to the local and attribute locations. The backbone network of LKWS (Yang et al., 2021) is based on PCB (Sun et al., 2018). In local feature extraction, the visibility label of points is generated by pose estimation and a reasonable threshold, and then the visibility of thick stripes is obtained by a voting mechanism. Based on the visibility of stripes, a visibility discriminator is trained to recognize noise interference. PGFA (Miao et al., 2019) introduces a two-branch structure, where the local branch extracts local features based on horizontal segmentation. The global branch is guided by pose, and key points are first obtained from pose estimation. Then, a reasonable threshold is set to filter the noise points, a proper dot product is performed with the feature map to fuse the features, and the features of the partial branches are stitched together into the final global features. Similarly, PDVM (Zhou et al., 2020b) extracts the de-observed global features based on the pose heat map. Segmentation guides local feature extraction.

4.1.2. Relationship Representation

By focusing on feature relationships, occlusions are handled in a suppressed, removed, or supervised manner. We divide them into attention, clustering, graph convolution, and shared region (see Figure 5) according to their different ways and means of learning relationships

Attention. By introducing the attention mechanism, the model can select the highly salient and discriminative regions to suppress the interference of noise.

To address the issue of missing images in person Re-ID, DPPR (Kim & Yoo, 2017) employs an attention mechanism to emphasize the same pedestrian part across different images. This approach enhances the representation of individuals and improves matching accuracy. Moreover, OCNet (Kim et al., 2022) mitigates the effect of noise by capturing higher-order relationships among regional features and incorporating them with weighted combinations. This method effectively suppresses the influence of noisy or irrelevant information, resulting in more robust and accurate person Re-ID outcomes. AACN (Xu et al., 2018) combines pose guided attention maps and partial visibility

scores to remove background distractions and occlusions before extracting clean pedestrian features. DAREID (Xu et al., 2021) introduces dual attention recognition. The local area visible to the pedestrian is obtained by gesture-guided spatial attention. Global features are extracted by feature activation and pose. Both will then be used together to guide the representation of features. PISNet (Zhao et al., 2020) is concerned with the overlapping area between people and objects. A module is designed to act as a guide feature by querying features, which can attenuate the problem of attention distraction caused by multiple pedestrians in the gallery. Also, a reverse attention module based on strong activation attention is designed, which enables the model to assign more weight to the target region. APN (Huo et al., 2021) proposes a partial perceptual attention network, which takes partial feature maps as query vectors, calculates a similarity mapping M with a mapping X of the feature maps, and morphs the features by weighting M by X to achieve the purpose of aggregating and extracting refined features. MHSA-Net (Tan et al., 2022a) multiplies attention weights with feature maps and applies a nonlinear transformation to encourage multi-headed attention mechanisms to adaptively capture key local features. CASN (Zheng et al., 2019) takes attention and attention consistency as the criteria for model learning and removes occlusion by introducing an attention twin network to focus on more discriminative core areas. VPM (Sun et al., 2019b) learns the visibility and location of components by introducing a self-supervised component localizer at the convolution output and introducing a feature extractor that generates region information through weighted pooling. PSE (Sarraz et al., 2018) solves the occlusion problem caused by view angle using view angle prediction.

Attention-based approaches not only enhance the flexibility of the model, but also inject more contextual information into the features. PAFM (Yang et al., 2022) introduces an improved spatial attention module to discover relationships between pixel points while capturing and aggregating pixel points with high semantic relevance. Finally, it is multiplied with the feature map containing pose information to perform feature fusion. Co-Attention (Lin & Wang, 2021) takes the analytic mask of a partial pedestrian image and whole image as the target and matches it through a self-attention mechanism (Li et al., 2020). Finally, noise interference is suppressed by focusing pedestrian features. QPM (Wang et al., 2022b) divides the feature map into six parts evenly in the vertical direction, and introduces a component quality score to judge the visibility. Meanwhile, a two-layer identity-aware module based on an attention map is used to deal with pedestrian occlusion in the global branch. Finally, global features are adaptively extracted from clean pedestrian regions. DSOP (Wang et al., 2020b) divides occlusion into shallow and deep layers. The shallow layer learns the feature after occlusion by focusing on the local region, and the deep layer gives a large receptive field to learn the global feature, that is, the feature before occlusion. After that, the channel and spatial attention mechanisms are

applied to the two branches for weighted fusion of features (Ning et al., 2021).

Clustering. The interference of noise is solved by finding the inherent distribution structure of the data to categorize the pixel points.

ISP (Zhu et al., 2020) assigns a pseudo-label to each pixel by tandem clustering. All pixels of the human body image are firstly divided into foreground and background, based on the assumption that the foreground is more responsive than the background. Secondly, the pixels are clustered into different parts and assigned pseudo-labels. Based on the pseudo-labels, different weights are assigned to the pixels to extract local features. This not only separates occlusions from pedestrians at the pixel level, but also enables automatic alignment.

Graph Convolution. By learning the high-order semantic relationship between pixels, the noise interference is suppressed by restricting the information transmission.

HOReID (Wang et al., 2020a) introduces a matrix describing the higher order relationships between points and later passes information in this relationship matrix to form a topological map. With the help of the constraints of the topological map, the transfer of useless information between points is suppressed, and the purpose of noise removal is achieved.

Shared Area. The interference of noise is reduced by sensing the same body parts of pedestrians in the image pairs to extract shareable features.

DPPR (Kim & Yoo, 2017) gives larger weights to regions containing the same body parts to improve the ability of the model to extract core features. VPM (Sun et al., 2019b) solves the alignment and denoising problem by perceiving the visibility of shared regions. PPCL (He et al., 2021b) learns component matching in a self-supervised manner and finally computes image similarity based on shared semantic corresponding regions only. KBFM (Han et al., 2020) focuses on extracting highly visible and shareable pose points, which are used as the core area to extract features for matching, and achieve the effect of denoising and alignment.

4.1.3. Other Methods

Regional reconfiguration. This is complements obscured or noisy areas by using complete pedestrian areas.

To solve the problem of information loss caused by occlusion, RFCNet (Hou et al., 2021) introduces an encoder–decoder that uses non-occlusion remote spatial context for feature completion. The encoder is modeled by similarity region assignment. The decoder reconstructs the occluded region by establishing the correlation between the occluded region and distant non-occluded region through clustering. ACSAP (He et al., 2021c) combines attitude and adversarial generation networks and designs an attitude-guided spatial generator and spatial discriminator to remove noise interference.

Data enhancement. The sensitivity of the model to occlusion is improved by incorporating transformation of the data.

APNet (Zhong et al., 2020a) proposes a method to modify the detected bounding box. APNet (Zhong et al., 2020a) designed a bounding box aligner that slides over the image in a matching manner. Then, a feature extractor with high discriminative power is designed to extract the core local features and discard the noisy local features. IGOAS (Zhao et al., 2021) adopts a progressive occlusion module, which randomly generates small uniform occlusion on a group of images and generates larger occlusion based on small occlusion after model learning. Such a growing occlusion region can improve the recognition ability of occlusion and achieve the purpose of removing occlusion noise. OAMN (Chen et al., 2021c) adopts a method based on cropping and scaling, predefines four corners, randomly selects a training image to be cropped and scaled to form patches on four positions, and realizes weighted learning in combination with attention to achieve denoising. RE (Zhong et al., 2020b) introduces the technique of random pixel removal, which replaces the pixel values in the region with random values by randomly selecting rectangular regions, thereby improving the diversity of data and robustness of the model. SSGR (Yan et al., 2021) introduces a compound batch erase method, which includes two erase operations: one is frequently used random erase, and the other is batch constant erase. It first divides the image horizontally into random S and randomly selects a strip in each sub-batch to erase. Then, referring to the self-attention mechanism and local feature learning, a matching-based disentanglement non-local operation is introduced to extract better features from the complete pedestrian region. ETNDNet (Dong et al., 2023) addresses the occlusion problem from an adversarial defence perspective. It deals with incomplete information, positional misalignment and noisy information through strategies of randomly erasing feature maps, introducing random transformations and perturbing feature maps.

Regularization. By imposing penalties and constraints on high-attention areas, the model is forced to focus on the full pedestrian area. Pedestrian features are extracted using complete information.

MHSA-Net (Tan et al., 2022a) introduces a feature regularization mechanism, which consists of a regularization term based on attention weight embedding and a hard triplet loss based on triplet feature units. The regularization term can cover local information in many ways and increase the completeness of information (Ning et al., 2020a). Hard triplet loss can refine the fusion and be better used for pedestrian matching.

Teacher-student model. Teacher models assist student models in dealing with occlusion problems.

HG (Kiran et al., 2021) designs an end-to-end unsupervised teacher-student framework that lets the teacher network learn the between-class distance by inputting different combinations of images, and then the student inherits the network and learns the within-class distance by inputting more noisy images of the same class. At the same time, the attention embedding method with distance distribution matching can help the student network to remove noise

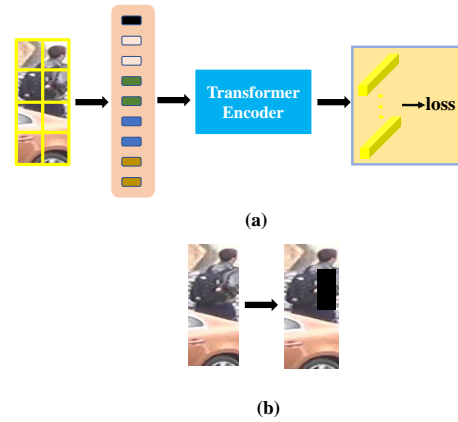


Figure 6: (a) Schematic of the transformer-based approach. (b) Schematic representation of data augmentation.

interference better and extract more discriminative features. AFPB (Zhuo et al., 2019) first puts regular data and pedestrian volume data simulating occlusion into the teacher network, and then it conducts joint training to make the teacher network learn a basic model that is robust to occlusion. The student network then inherits the teacher network. It learns on more realistic, noisier real-world occluded pedestrian data.

Multiscale. The occlusion problem is handled by multi-scale feature representation.

DSR (He et al., 2018) focuses on solving problems caused by differences in scale. DSR (He et al., 2018) first trains a fixed-size fully convolutional network with only convolution and pooling on Market-1501 (Zheng et al., 2015a) to represent the identity feature map, and it then introduces three different scales of blocks to extract features in a sliding manner (Li et al., 2021). Similarly, FPR (He et al., 2019) also introduces a structure that only has convolution and pooling and proposes a pyramid layer composed of multiple different pooling kernels to solve the scale problem, an attention-based foreground probability generator to process the background, and a small weight to the background to achieve removal of background distractions.

4.2. Based on vit

TransReID (He et al., 2021a), proposed in 2021, is the first model to apply a vit (Dosovitskiy et al., 2020) in ReID (see Figure 6), which has two major features compared to ResNet (He et al., 2016): (1) Multi-headed self-attention is better at capturing long-range relationships and driving the model to focus on different body parts (Khan et al., 2022; Shamshad et al., 2023). (2) The transformer can retain more detailed information in the absence of downsampling computation. Based on these characteristics, many variants of transformer have appeared in recent years, and researchers have widely used them in occlusion Re-ID.

PFD (Wang et al., 2022d) first divides the image into fixed-size blocks that can be overlapped and then uses the transformer encoder to capture contextual relationships.

Next, pose guided feature aggregation and a feature matching mechanism are used to display the visible body parts. Finally, the pose heat map and decoder are used as keys and values to learn a set of semantic part views to enhance the discriminability of body parts. DPM (Tan et al., 2022b) introduces subspace selection to deal with the alignment problem. Specifically, DPM (Tan et al., 2022b) first aggregates the feature representations of the overall prototype map and the occlusion map using hierarchical semantic information to enhance the quality of the generated prototype mask. Then, a head enrichment module based on normalization and orthogonality constraints is introduced to enhance the discriminative representation of features and remove the interference of noise. PFT (Zhao et al., 2022) introduces a learnable enhancement patch to compensate for the problem of local feature extraction (Islam, 2022) by transformer. Through feature slicing, merging, and stitching, the patch sequence can learn the long-range correlation of regions while ensuring the receptive field and paying more attention to local features. FED (Wang et al., 2022g) divides occlusion into non-pedestrian and non-target pedestrian occlusion, and focuses on the latter. Specifically, an occlusion set is first created to enhance the data. Then, a multiplicative occlusion score is introduced to diffuse the visible pedestrian parts, which improves the quality of the synthesized non-target pedestrians. The joint optimization of feature erasure and feature diffusion modules realizes the perception ability of the model to the target pedestrian.

FRT (Xu et al., 2022) first classifies the pedestrian into head, torso, and legs using a pretrained pose estimation model HRNet (Sun et al., 2019a), and extracts the corresponding features. Then the occlusion elimination module based on graph matching is introduced to eliminate the interference caused by occlusion by learning the similarity of common regions. Finally, FRT (Xu et al., 2022) recovers query features by aggregating neighbor features to solve the problem of information loss caused by occlusion. TL-TransNet (Wang et al., 2022c) uses a well-improved Swin transformer (Liu et al., 2021) as a benchmark model to capture the main part of the person and uses DeepLabV3+ (Chen et al., 2018) to remove background interference in the query and gallery. Finally, a reordering method based on hybrid similarity and background adaptation is designed to achieve the fusion of original features and removed background features. PADE (Huang et al., 2022) first obtains two new images through cropping and erasing operations and feeds them together with the original image into a multi-branch parameter sharing network with a vit (Dosovitskiy et al., 2020) as the backbone to enhance the global and local features in a manner similar to the self-attention mechanism. Finally, they are connected to form the final feature representation.

4.3. Composite Method

By introducing more than two different networks, the occlusion problem is dealt with in an interactive or fused manner.

FGMFN (Zhang et al., 2022a) introduces a dual branch network. The local feature branches are first passed through an affine transformation based on ResNet18. Then, input into ResNet50 (He et al., 2016) to get the upper body features and divide it into three regions, while introducing the attention module based on the gate mechanism to remove noise interference. The global feature branch adopts a feature extraction scheme based on block partition, and finally, the features of the two branches are fused proportionally as the final feature. Pirt (Ma et al., 2021) first pre-trains the HRNet (Sun et al., 2019a) pose estimation model on the COCO (Lin et al., 2014) dataset, from which a two-branch structure is elicited. Intra-part features are guided by a carefully modified ResNet50 (He et al., 2016), inter-part relationships are guided by a transformer, and the effects of occlusion are removed by establishing part-aware long-range dependencies. Pirt (Ma et al., 2021) learns inter- and intra-part relationships in a collaborative manner. MAT (Zhou et al., 2022) first uses a CNN to extract features from the image. Then, it flattens and passes them to a transformer. This method uses the methods of feature map and key point embedding to obtain a key point heat map and segmentation map. It uses affine transformation to obtain motion information of each key point and combines action information to realize fine-grained human body segmentation, and extracts representative pedestrian body parts to remove interference noise. DRL-Net (Jia et al., 2022) first acquires obstacles from the training images to construct augmented samples with random obstacles. Then, a CNN and Transformer are concatenated to design a query-based semantic feature extraction layer. Finally, the semantic bootstrap is used to learn positive and negative sample comparisons and remove interference noise.

4.4. 3D Re-ID

Compared to 2D, the use of 3D information for occlusion person Re-ID is a relatively new approach. The shape and spatial depth features represented by 3D data are robust to texture information, and it usually reduces the interference caused by occlusion through 3D feature denoising, 3D feature complementation and multi-view construction.

PersonX (Sun & Zheng, 2019) constructs virtual 3D models by scanning people and objects in the real world and then maps them back to 2D for re-representation. Such manipulation of the data enhances the data representation. (Wang et al., 2022f) used UV texture mapping to clone clothing from real-world pedestrians to virtual 3D characters, while using a patch-based feature segmentation and expansion approach to deal with occlusion. A more common form of 3D information is the point cloud (Qi et al., 2017), where the depth information in the point cloud can be used as an additional channel to the image. OG-Net (Zheng et al., 2022) uses Skinned Multi-Person Linear (SMPL (Kanazawa et al., 2018)) to generate six channels of point cloud data from 2D images, providing positional and texture information.

ASSP (Chen et al., 2021b) uses 3D body reconstruction as an auxiliary task for 2D feature extraction. Specifically,

texture-insensitive 3D shape information is first extracted from 2D images as auxiliary features. After that, a 3D row human model is created using SMPL (Loper et al., 2015), while an adversarial learning and self-supervised projection combination is designed to combine 2D and 3D information into a 3D model for reconstruction (Ning et al., 2020b). Regularization based on 3D reconstruction forces the model to decouple 3D shape information from visual features and remove the interference of noise to extract more discriminative features. JGCL (Chen et al., 2021a) mitigates the lack of information caused by perspective in an unsupervised mapping. Specifically, a corresponding 3D mesh is first generated using a 3D network generator HMR (Kanazawa et al., 2018). After that, the model is rotated and combined with a GAN to generate diverse views of the human body. These generated new views are combined with the original images in contrast learning while enhancing the view-invariant representation to improve the generated picture quality. 3DT (Zhang et al., 2022c) implements group person Re-ID using a 3D transformer. Because pedestrians in a group inevitably occlude each other, it transforms the 3D space into a discrete space by introducing a spatial layout token based on quantization and sampling, and it later assigns layout features to each member to reconstruct the spatial relationships between members.

However, the research on recognition using point clouds is still limited compared to 2D images, which is an important research direction for the future.

4.5. Multi-modal Re-ID

RGB-IR multimodal Re-ID. Both day and night are important scenes of pedestrian life, and in the case of insufficient illumination, images can only be collected by infrared cameras (Nguyen et al., 2017; Wu et al., 2017b). If there is occlusion in the scene, the infrared image still has occlusion. At the same time, the infrared image can be used as a special channel of the RGB image, which makes the representation mode of the RGB image more complete and can supplement the information well in the case of information loss caused by occlusion. The RGB-IR multimodal Re-ID is designed to feed both infrared and conventional images into the model. Removal of interference from occlusion is achieved by the relationship of different modalities or by combining approaches, such as attention mechanisms, in dealing with single modal noise, multi-scale, etc.

DDAG (Ye et al., 2020) proposes a dynamic dual attention cross-modal graph structure. First, local attention is generated according to the similarity between features. Then, an aggregation representation of part-level relation learning is introduced. At the same time, the graph structure is introduced to remove the interference of noise based on relation. MSPAC (Zhang et al., 2021) proposes a multi-scale-based component awareness mechanism. By adding an attention mechanism at the single scale, more fine-grained features are extracted in channel and spatial dimensions. After that, feature aggregation is realized using a cascade

framework. By adding different scale features, the global structured body information is represented uniformly. CM-LSP-GE (Wang et al., 2022e) is a framework for global features and local characteristics. The occlusion problem is solved by local features, and the alignment problem is solved by image segmentation and computing the shortest path of local features in two images.

To solve the intra-modal problem, HMML (Zhang et al., 2022b) introduces a pairing-based intra-modal similarity constraint to enhance the features. Similarly, CMC (Wen et al., 2022) introduces multi-scale, multi-level feature learning to achieve refined feature extraction. To solve the problem of pedestrian pose misalignment caused by occlusion in transmembrane state, DAPN (Liu et al., 2022) proposes an alignment network that can learn global and local modal invariance. Specifically, DAPN (Liu et al., 2022) first introduces an adaptive spatial transform module to align images. Second, the image is segmented horizontally to extract local features. Meanwhile, to learn the similarity representation of different modes, the different modes are embedded into a unified feature space (Cai et al., 2021). Finally, the global and local features are fused as the final features. To solve the alignment problem, SPOT (Chen et al., 2022) proposes a transformer-based network. First, a relational network composed of four convolution layers and two pooling layers is used to process the human body key point heat map to obtain the pedestrian body structure information. Combining it with the attention mechanism, the pedestrian region is highlighted to remove the background interference. Then, the transformer is used to mine the relationship between parts' positions and features to enhance the discriminability of local features. The final feature is extracted by adding weight combination. VI (Park et al., 2021) first extracts features of IR and RGB using a dual-stream CNN. The cosine similarity of all corresponding feature pairs is calculated simultaneously, and the corresponding matching probability is calculated by the SoftMax function. These probabilities are taken as semantic similarity features of different modalities. Then, more discriminative features are extracted by local feature association. The above features are then aggregated to form the final feature. To solve the problem of image internal misalignment, DTRM (Ye et al., 2021a) combines attention and partial aggregation, and uses the context relationship of the two modalities to improve the global features to eliminate the noise effect.

RGB-Depth multimodal Re-ID. Depth (Wang et al., 2021a) images are captured through devices such as laser radars, and they provide body shape and skeletal information by measuring distance. For images, when information is lost owing to obstacles, depth features can supplement the position information of texture features to assist in a more complete expression. At the same time, it can solve the lighting problem and the problem of changing clothes for pedestrians. It can also help solve the problems of obstacle illumination and different changing environments for clothing. RGB-Depth multimodal Re-ID aims to input depth map

Table 2

Comparison of experimental results based on local feature learning methods. The red numbers indicate the best results. (in %).

Method		Venue	Occluded-Duke		Occluded-REID		Partial-REID		Partial-iLIDS		Market1501		DukeMTMC-reID		
			Rank-1	mAP	Rank-1	mAP	Rank-1	Rank-3	Rank-1	Rank-3	Rank-1	mAP	Rank-1	mAP	
Local Feature Learning	Body Segmentation	CBDB-Net (Tan et al., 2021)	TCSVT2021	50.09	38.9	-	-	66.7	78.3	68.4	81.5	94.4	85	87.7	74.3
		OCNet (Kim et al., 2022)	ICASSP2022	64.30	54.40	-	-	-	-	-	-	95	89.3	90.5	80.2
	Pose Estimation	AACN (Xu et al., 2018)	CVPR2018	-	-	-	-	-	-	-	88.69	82.96	76.84	59.25	-
		ACSAP (He et al., 2021c)	ICIP2021	-	-	-	-	77	83.7	76.5	87.4	-	-	-	-
		DAREID (Xu et al., 2021)	KBS2021	63.4	-	-	-	68.1	79.5	76.7	85.3	94.6	87	88.9	78.4
		DSA-reID (Zhang et al., 2019)	CVPR2019	-	-	-	-	-	-	-	-	95.7	87.6	86.2	74.3
		HOReID (Wang et al., 2020a)	CVPR2020	-	-	80.3	70.2	85.3	91	72.6	86.4	94.2	84.9	86.9	75.6
		PAFM (Yang et al., 2022)	NCA2022	55.1	42.3	76.4	68	82.5	-	-	-	95.6	88.5	91.2	80.1
		PDC (Su et al., 2017)	ICCV2017	-	-	-	-	-	-	-	-	84.14	63.41	-	-
		PGFL-KD (Zheng et al., 2021)	MM2021	63	54.1	80.7	70.3	85.1	90.8	74	86.7	95.3	87.2	89.6	79.5
		PGMANet (Zhai et al., 2021)	IJCNN2021	-	-	-	-	82.1	85.5	68.8	78.1	-	-	-	-
		PMFB (Miao et al., 2021)	TNNLS2021	56.3	43.5	-	-	72.5	83	70.6	81.3	92.7	81.3	86.2	72.6
	PVPM (Gao et al., 2020b)	CVPR2020	-	-	70.4	61.2	78.3	-	-	-	-	-	-	-	
	Semantic Segmentation	Co-Attention (Lin & Wang, 2021)	ICIP2021	-	-	-	-	83	90.3	73.1	83.2	-	-	-	-
		HPNet (Huang et al., 2020)	ICME2020	-	-	87.3	77.4	85.7	-	68.9	80.7	-	-	-	-
		MMGA (Cai et al., 2019)	CVPR2019	-	-	-	-	-	-	-	-	95	87.2	89.5	78.1
		SGSFA (Ren et al., 2020)	PMLR2020	62.3	47.4	63.1	53.2	68.2	-	-	-	92.3	80.2	84.7	70.8
		SORN (Zhang et al., 2020)	TCSVT2020	57.6	46.3	-	-	76.7	84.3	79.8	86.6	94.8	84.5	86.9	74.1
	SPReID (Kalayeh et al., 2018)	CVPR2017	-	-	-	-	-	-	-	-	94.63	90.96	88.96	84.99	
	Attribute Annotation	ASAN (Jin et al., 2021)	TCSVT2021	55.40	43.80	82.50	71.80	86.80	93.50	81.70	88.30	94.60	85.30	87.50	76.30
Mixing Method	FGSA (Zhou et al., 2020a)	TIP2020	-	-	-	-	-	-	-	-	91.50	85.40	85.90	74.10	
	GASM (He & Liu, 2020)	ECCV2020	-	-	80.30	73.10	-	-	-	-	95.30	84.70	88.30	74.40	
	PGFA (Miao et al., 2019)	ICCV2019	-	-	-	-	68.80	80.00	69.10	80.90	91.20	76.80	82.60	65.50	
	SSPreID (Quispe & Pedrini, 2019)	IVC 2019	-	-	-	-	-	-	-	-	93.70	90.80	86.40	83.70	
	LKWS (Yang et al., 2021)	ICCV2021	62.2	46.3	81	71	85.7	93.7	80.7	88.2	-	-	-	-	
TSA (Gao et al., 2020a)	ACM MM2020	-	-	-	-	72.70	85.20	73.90	84.70	-	-	-	-		

and RGB image simultaneously, and remove the interference of noise by the attention mechanism and other methods.

CMD (Hafner et al., 2022) proposes an approach combining embedding representation and feature distillation. It removes noise through a gate-controlled attention mechanism. This mechanism uses one modality to dynamically activate the more discriminative features in another modality by gating signals.

RGB-Text multimodal Re-ID. RGB-Text multimodal Re-ID aims to introduce text data to enhance feature representation by sharing semantic information and attentional calibration to eliminate the effect of noise. In daily life, text information is one of the most frequently used types of information. When image information is missing or cannot be used owing to obstacles, it can be supplemented with text.

AXM-Net (Farooq et al., 2022) dynamically exploits multi-scale information of text and images, recalibrating each modality according to the shared semantics and adding contextual attention to the text branch to supplement the information of the convolution block. Furthermore, attention is introduced to enhance feature consistency and local information of the visual part. It can learn the alignment semantic information of different modalities and automatically remove the interference of irrelevant information.

5. Method Comparison

We statistically evaluate the results of the occluded person Re-ID methods on two general datasets (Market1501 (Zheng et al., 2015a), DukeMTMC-reID (Ristani et al., 2016)), two occluded person Re-ID datasets (Occluded-DukeMTMC (Miao et al., 2019), Occluded-REID (Zheng et al., 2015b)) and two partial person Re-ID datasets (Partial-ReID (Zheng et al., 2015b), Partial-iLIDS (He et al., 2018)).

We simply divide them into three categories: The experimental results based on the local feature learning method are shown in Table 2. It contains body segmentation, pose estimation, semantic segmentation, attribute annotation, and mixing method. The experimental results based on the relationship representation method are shown in Table 3. It contains shared area, clustering, figure convolution, and attention. The experimental results of other methods are shown in Table 4. It contains the transformer, mixing method, multi-scale, regional reconfiguration, data enhancement, and regularization. For an introduction to each class of methods and details of each study, the reader is referred to Section 4.

From the results we can get the following information: (1) From the results we can get the following information: OCNet (Kim et al., 2022) based on local feature learning, QPM (Wang et al., 2022b) based on relational representation, DPM (Tan et al., 2022b) and PFD (Wang et al., 2022d) based on transformer perform better on the Occluded-DukeMTMC dataset. On the Occluded-REID dataset, HPNet (Huang et al., 2020) based on local feature learning, HOReID (Wang et al., 2020a) based on relational representation, FED (Wang et al., 2022g) and PFD (Wang et al., 2022d) based on transformer perform stably. On the Partial-ReID dataset, ASAN (Jin et al., 2021) and LKWS (Yang et al., 2021) based on local feature learning, MHSA-Net (Tan et al., 2022a) based on relational representation, and FRT (Xu et al., 2022) based on transformer achieve better performance. On the Partial-iLIDS dataset, ASAN (Jin et al., 2021) based on local feature learning, MHSA-Net (Tan et al., 2022a) and QPM (Wang et al., 2022b) based on relational representation, ACSAP (He et al., 2021c) based on region reconstruction, and OAMN (Chen et al., 2021c) based on data augmentation achieve very stable performance. Therefore, there is no single method that achieves

Table 3

Comparison of experimental results based on relationship representation methods. The red numbers indicate the best results.(in %).

Method		Venue	Occluded-Duke		Occluded-REID		Partial-REID		Partial-iLIDS		Market1501		DukeMTMC-reID		
			Rank-1	mAP	Rank-1	mAP	Rank-1	Rank-3	Rank-1	Rank-3	Rank-1	mAP	Rank-1	mAP	
Relationship Representation	Shared Area	KBFM (Han et al., 2020)	ICIP2020	-	-	-	-	69.7	82.2	64.1	73.9	-	-	-	-
		PPCL (He et al., 2021b)	CVPR2021	-	-	-	-	83.70	88.70	71.40	85.70	-	-	-	-
		VPM (Sun et al., 2019b)	CVPR2019	-	-	-	-	67.70	81.90	65.50	74.80	90.40	75.70	-	-
	Clustering	ISP (Zhu et al., 2020)	ECCV2020	62.80	52.30	-	-	-	-	-	-	94.63	90.69	88.96	84.99
	Figure Convolution	HORelD (Wang et al., 2020a)	CVPR2020	-	-	80.3	70.2	85.3	91	72.6	86.4	94.2	84.9	86.9	75.6
	Attention	AACN (Xu et al., 2018)	CVPR2018	-	-	-	-	-	-	-	-	88.69	82.96	76.84	59.25
		APN (Huo et al., 2021)	ICPR2021	-	-	-	-	71.80	85.50	66.40	76.50	96.00	89.00	89.50	79.20
		CASN (Zheng et al., 2019)	CVPR2019	-	-	-	-	-	-	-	-	94.40	82.80	87.70	73.70
		Co-Attention (Lin & Wang, 2021)	ICIP2021	-	-	-	-	83.00	90.30	73.10	83.20	-	-	-	-
		DARelD (Xu et al., 2021)	KBS2021	63.4	-	-	-	68.1	79.5	76.7	85.3	94.6	87	88.9	78.4
		DSOP (Wang et al., 2020b)	JPCS2020	57.70	45.30	-	-	-	-	-	-	95.40	85.90	88.20	77.00
		MHSA-Net (Tan et al., 2022a)	TNNLS2022	59.70	44.80	-	-	85.70	91.30	74.90	87.20	95.50	93.00	90.70	87.20
		OCNet (Kim et al., 2022)	ICASSP2022	64.30	54.40	-	-	-	-	-	-	-	-	-	-
		PAFM (Yang et al., 2022)	NCA2022	55.1	42.3	76.4	68	82.5	-	-	-	95.6	88.5	91.2	80.1
		PISNet (Zhao et al., 2020)	ECCV2020	-	-	-	-	-	-	-	-	95.60	87.10	88.80	78.70
PSE (Sarfranz et al., 2018)		CVPR2018	-	-	-	-	-	-	-	-	90.30	84.00	85.20	79.80	
QPM (Wang et al., 2022b)		ITM2022	64.40	49.70	-	-	81.70	88.00	77.30	85.70	-	-	-	-	
VPM (Sun et al., 2019b)	CVPR2019	-	-	-	-	67.70	81.90	65.50	74.80	90.40	75.70	-	-		

Table 4

Comparison of experimental results with other methods. The red numbers indicate the best results.(in %).

Method		Venue	Occluded-Duke		Occluded-REID		Partial-REID		Partial-iLIDS		Market1501		DukeMTMC-reID	
			Rank-1	mAP	Rank-1	mAP	Rank-1	Rank-3	Rank-1	Rank-3	Rank-1	mAP	Rank-1	mAP
Transformer	DPM (Tan et al., 2022b)	ACM MM 2022	71.40	61.80	85.50	79.70	-	-	-	-	95.50	89.70	91.00	82.60
	FED (Wang et al., 2022g)	CVPR2022	68.10	56.40	86.30	79.30	83.10	-	-	-	95.00	86.30	89.40	78.00
	FRT (Xu et al., 2022)	TIP2022	70.70	61.30	80.40	71.00	88.20	93.20	73.00	87.00	95.50	88.10	90.50	81.70
	TransRelD (He et al., 2021a)	ICCV2021	66.40	59.20	-	-	-	-	-	-	95.20	88.90	90.70	82.00
	PFD (Wang et al., 2022d)	AAAI2022	69.50	61.80	81.50	83.00	-	-	-	-	95.50	89.70	91.20	83.20
PFT (Zhao et al., 2022)	NCA2022	69.80	60.80	83.00	78.30	81.30	79.90	68.10	81.50	95.30	88.80	90.70	82.10	
Mixing Method	DRL-Net (Jia et al., 2022)	TMM2021	65.80	53.90	-	-	-	-	-	-	94.70	86.90	88.10	76.60
	Pirt (Ma et al., 2021)	ACMMM2021	60.00	50.90	-	-	-	-	-	-	94.10	86.30	88.90	77.60
Multiscale	DSR (He et al., 2018)	CVPR2018	40.80	30.40	72.80	62.80	50.70	70.00	58.80	67.20	83.58	64.25	-	-
	FPR (He et al., 2019)	ICCV2019	-	-	78.30	68.00	81.00	-	68.10	-	95.42	86.58	88.64	78.42
Regional Reconfiguration	ACSAP (He et al., 2021c)	ICIP2021	-	-	-	-	77.00	83.70	76.50	87.40	-	-	-	-
	RFCNet (Hou et al., 2021)	TPAMI2021	63.90	54.50	-	-	-	-	-	-	95.20	89.20	90.70	80.70
Data Enhancement	IGOAS (Zhao et al., 2021)	TIP2021	60.10	49.40	81.10	-	-	-	-	-	93.40	84.10	86.90	75.10
	OAMN (Chen et al., 2021c)	ICCV2021	62.60	46.10	-	-	86.00	-	77.30	-	93.20	79.80	86.30	72.60
	SSGR (Yan et al., 2021)	ICCV2021	65.80	57.20	78.50	72.90	-	-	-	-	96.10	89.30	91.10	81.30
Regularization	MHSA-Net (Tan et al., 2022a)	TNNLS2022	59.70	44.80	-	-	85.70	91.30	74.90	87.20	95.50	93.00	90.70	87.20

the best performance on all datasets. (2) In general, the performance on the occlusion dataset reflects the ability of the model to resist noise, the performance on the partial dataset reflects the recognition ability of the model under the condition of missing pedestrian information, and the performance on the general dataset reflects the comprehensive performance of the model. Each of these approaches addresses one or more specific problems. (3) Attention and pose estimation are the more mainstream and typical of the many pedestrian re-identification methods for dealing with occlusion. Attribute annotation-based, clustering-based, figure convolution-based and regularisation-based methods, on the other hand, have received less attention.

6. Future directions

6.1. Richer, higher quality datasets

Most models are evaluated on datasets collected in controlled environments. The data in real-world scenarios is

often uncontrollable, which can significantly impact the model's performance on such datasets.

For an occluded person Re-ID dataset, it is necessary to incorporate one or more modal inputs, including a diverse combination of images, text, infrared maps, and depth maps. This enables the model to effectively handle a wider range of realistic occlusion scenarios. Moreover, there is a lack of larger datasets encompassing a broader range of domains, environments (Gou et al., 2018), and higher resolutions, which would provide richer content and higher quality for research purposes.

6.2. More robust and varied feature extraction

3D Re-ID. Inspired by human three-dimensional cognition, some researchers believe that the complete pedestrian representation should be a fusion of 3D and 2D (Zheng et al., 2022).

At present, PointNet (Qi et al., 2017), as a representative of deep learning methods in point cloud feature extraction (Wang et al., 2022a; CS et al., 2022), has demonstrated

promising results. Point cloud completion (Fei et al., 2022) and point cloud correction can aid in 3D occluded person Re-ID, while 3D pose estimation (Wang et al., 2021b) and 3D semantic segmentation (Xie et al., 2020) can guide the feature extraction process for person Re-ID. However, research in the 3D domain for pedestrian recognition (Zhao et al., 2013; Sun et al., 2019b) is still relatively limited compared to the advancements in 2D approaches. Therefore, 3D occluded person Re-ID represents a significant and promising research direction for the future (Tirkolaee et al., 2020).

Multimodal Re-ID. The information captured from different modalities demonstrates a significant diversity in content representation (Wu et al., 2017b,a). Improving the interaction, fusion, and extraction of more comprehensive pedestrian features at both the data and feature extraction stages represents a crucial research direction for future advancements (Tutsoy & Tanrikulu, 2022; Sekhar et al., 2017).

Cross-resolution occluded person Re-ID. Owing to the influence of the distance and pixel size of the collection device, the resolution of the collected samples is uneven, and the feature space correspondence is also inconsistent (Li et al., 2019). At the same time, low resolution will lose significant spatial and detail information (Mao et al., 2019). How to extract pedestrian features at different resolutions under occlusion conditions is a problem to be solved in the future.

Fast response, smaller occlusion person Re-ID model. Constructing smaller (Zhou et al., 2019; Li et al., 2018) and faster (Liu et al., 2017) occluded person Re-ID models with reduced parameters is a crucial research direction for future advancements (Tutsoy et al., 2018).

Unsupervised and semi-supervised occluded person Re-ID. The complex manual labeling process is omitted, and the pedestrian features are learned by using the datasets without labels (Zhang & Lu, 2018; Liu et al., 2019) or with a small number of labels (Wang et al., 2019c,a; Nagaraju et al., 2016).

Currently, the performance of unsupervised and semi-supervised based methods on the task of occluded person Re-ID is still some way off compared to supervised methods. Supervised methods usually rely on large-scale labelled datasets for training and thus can achieve high performance. However, as unsupervised and semi-supervised methods are increasingly studied, they show significant potential in improving the generalisation of occluded person Re-ID models.

6.3. Occluded person Re-ID system

At present, few researchers combine object detection and occluded person Re-ID together. The end-to-end person Re-ID systems are lacking, and the integrated system has more applications in real life (Martinel et al., 2016). How to combine the two more effectively and rationally and design a occluded person Re-ID system that is more robust to occlusion is an important research direction.

7. Conclusion

This review offers a comprehensive and integrated analysis and discussion of deep learning methods for occluded person Re-ID, addressing both practical and research-driven requirements. Firstly, we introduce the classification of occlusion problems and the datasets specifically designed for occluded person Re-ID. Secondly, we comprehensively classify and introduce the methods proposed in top international journals and conferences before 2023 for addressing occluded person Re-ID. Finally, the future prospects of occluded person Re-ID are analyzed from data, feature, and system perspectives, respectively. In this study, we categorize the most significant image feature extraction methods into five major categories: local feature learning, relational representation, transformer-based methods, mixing methods, and other approaches. This review will assist researchers in comprehending the process and objectives of these methods, providing valuable references and contributing to the research significance in the advancement of occluded Re-ID.

References

- Bedagkar-Gala, A. & Shah, S. K. (2014). A survey of approaches and trends in person re-identification. *Image and vision computing*, 32(4), 270–286.
- Cai, H., Wang, Z., & Cheng, J. (2019). Multi-scale body-part mask guided attention for person re-identification. In *Proceedings of the IEEE/CVF Conference on Computer Vision and Pattern Recognition Workshops* (pp. 0–0).
- Cai, X., Liu, L., Zhu, L., & Zhang, H. (2021). Dual-modality hard mining triplet-center loss for visible infrared person re-identification. *Knowledge-Based Systems*, 215, 106772.
- Chen, C., Ye, M., Qi, M., Wu, J., Jiang, J., & Lin, C.-W. (2022). Structure-aware positional transformer for visible-infrared person re-identification. *IEEE Transactions on Image Processing*, 31, 2352–2364.
- Chen, H., Wang, Y., Lagadec, B., Dantcheva, A., & Bremond, F. (2021a). Joint generative and contrastive learning for unsupervised person re-identification. In *Proceedings of the IEEE/CVF conference on computer vision and pattern recognition* (pp. 2004–2013).
- Chen, J., Jiang, X., Wang, F., Zhang, J., Zheng, F., Sun, X., & Zheng, W.-S. (2021b). Learning 3d shape feature for texture-insensitive person re-identification. In *Proceedings of the IEEE/CVF Conference on Computer Vision and Pattern Recognition* (pp. 8146–8155).
- Chen, L.-C., Zhu, Y., Papandreou, G., Schroff, F., & Adam, H. (2018). Encoder-decoder with atrous separable convolution for semantic image segmentation. In *Proceedings of the European conference on computer vision (ECCV)* (pp. 801–818).
- Chen, P., Liu, W., Dai, P., Liu, J., Ye, Q., Xu, M., Chen, Q., & Ji, R. (2021c). Occlude them all: Occlusion-aware attention network for occluded person re-id. In *Proceedings of the IEEE/CVF international conference on computer vision* (pp. 11833–11842).
- Cheng, D. S., Cristani, M., Stoppa, M., Bazzani, L., & Murino, V. (2011). Custom pictorial structures for re-identification. In *Bmvc*, volume 1 (pp. 6): Citeseer.
- CS, W., H, W., X, N., SW, T., & WJ, L. (2022). 3d point cloud classification method based on dynamic coverage of local area. *Journal of Software*, (pp. 0–0).
- Dong, N., Zhang, L., Yan, S., Tang, H., & Tang, J. (2023). Erasing, transforming, and noising defense network for occluded person re-identification. *arXiv preprint arXiv:2307.07187*.
- Dosovitskiy, A., Beyer, L., Kolesnikov, A., Weissenborn, D., Zhai, X., Unterthiner, T., Dehghani, M., Minderer, M., Heigold, G., Gelly, S., et al. (2020). An image is worth 16x16 words: Transformers for image recognition at scale. *arXiv preprint arXiv:2010.11929*.

- Ess, A., Leibe, B., Schindler, K., & Van Gool, L. (2008). A mobile vision system for robust multi-person tracking. In *2008 IEEE Conference on Computer Vision and Pattern Recognition* (pp. 1–8).: IEEE.
- Farooq, A., Awais, M., Kittler, J., & Khalid, S. S. (2022). Axm-net: Implicit cross-modal feature alignment for person re-identification. In *Proceedings of the AAAI Conference on Artificial Intelligence*, volume 36 (pp. 4477–4485).
- Fei, B., Yang, W., Chen, W.-M., Li, Z., Li, Y., Ma, T., Hu, X., & Ma, L. (2022). Comprehensive review of deep learning-based 3d point cloud completion processing and analysis. *IEEE Transactions on Intelligent Transportation Systems*.
- Fu, J., Liu, J., Tian, H., Li, Y., Bao, Y., Fang, Z., & Lu, H. (2019). Dual attention network for scene segmentation. In *Proceedings of the IEEE/CVF conference on computer vision and pattern recognition* (pp. 3146–3154).
- Gao, L., Zhang, H., Gao, Z., Guan, W., Cheng, Z., & Wang, M. (2020a). Texture semantically aligned with visibility-aware for partial person re-identification. In *Proceedings of the 28th ACM International Conference on Multimedia* (pp. 3771–3779).
- Gao, S., Wang, J., Lu, H., & Liu, Z. (2020b). Pose-guided visible part matching for occluded person reid. In *Proceedings of the IEEE/CVF conference on computer vision and pattern recognition* (pp. 11744–11752).
- Gou, M., Wu, Z., Rates-Borras, A., Camps, O., Radke, R. J., et al. (2018). A systematic evaluation and benchmark for person re-identification: Features, metrics, and datasets. *IEEE transactions on pattern analysis and machine intelligence*, 41(3), 523–536.
- Güler, R. A., Neverova, N., & Kokkinos, I. (2018). Densepose: Dense human pose estimation in the wild. In *Proceedings of the IEEE conference on computer vision and pattern recognition* (pp. 7297–7306).
- Hafner, F. M., Bhuyian, A., Kooij, J. F., & Granger, E. (2022). Cross-modal distillation for rgb-depth person re-identification. *Computer Vision and Image Understanding*, 216, 103352.
- Han, C., Gao, C., & Sang, N. (2020). Keypoint-based feature matching for partial person re-identification. In *2020 IEEE International Conference on Image Processing (ICIP)* (pp. 226–230).: IEEE.
- He, K., Zhang, X., Ren, S., & Sun, J. (2016). Deep residual learning for image recognition. In *Proceedings of the IEEE conference on computer vision and pattern recognition* (pp. 770–778).
- He, L., Liang, J., Li, H., & Sun, Z. (2018). Deep spatial feature reconstruction for partial person re-identification: Alignment-free approach. In *Proceedings of the IEEE conference on computer vision and pattern recognition* (pp. 7073–7082).
- He, L. & Liu, W. (2020). Guided saliency feature learning for person re-identification in crowded scenes. In *Computer Vision—ECCV 2020: 16th European Conference, Glasgow, UK, August 23–28, 2020, Proceedings, Part XXVIII 16* (pp. 357–373).: Springer.
- He, L., Wang, Y., Liu, W., Zhao, H., Sun, Z., & Feng, J. (2019). Foreground-aware pyramid reconstruction for alignment-free occluded person re-identification. In *Proceedings of the IEEE/CVF international conference on computer vision* (pp. 8450–8459).
- He, S., Luo, H., Wang, P., Wang, F., Li, H., & Jiang, W. (2021a). Transreid: Transformer-based object re-identification. In *Proceedings of the IEEE/CVF international conference on computer vision* (pp. 15013–15022).
- He, T., Shen, X., Huang, J., Chen, Z., & Hua, X.-S. (2021b). Partial person re-identification with part-part correspondence learning. In *Proceedings of the IEEE/CVF Conference on Computer Vision and Pattern Recognition* (pp. 9105–9115).
- He, Y., Yang, H., & Chen, L. (2021c). Adversarial cross-scale alignment pursuit for seriously misaligned person re-identification. In *2021 IEEE International Conference on Image Processing (ICIP)* (pp. 2373–2377).: IEEE.
- Hou, R., Ma, B., Chang, H., Gu, X., Shan, S., & Chen, X. (2021). Feature completion for occluded person re-identification. *IEEE Transactions on Pattern Analysis and Machine Intelligence*, 44(9), 4894–4912.
- Huang, H., Chen, X., & Huang, K. (2020). Human parsing based alignment with multi-task learning for occluded person re-identification. In *2020 IEEE international conference on multimedia and expo (ICME)* (pp. 1–6).: IEEE.
- Huang, H., Zheng, A., Li, C., He, R., et al. (2022). Parallel augmentation and dual enhancement for occluded person re-identification. *arXiv preprint arXiv:2210.05438*.
- Huo, L., Song, C., Liu, Z., & Zhang, Z. (2021). Attentive part-aware networks for partial person re-identification. In *2020 25th International Conference on Pattern Recognition (ICPR)* (pp. 3652–3659).: IEEE.
- Islam, K. (2022). Recent advances in vision transformer: A survey and outlook of recent work. *arXiv preprint arXiv:2203.01536*.
- Jia, M., Cheng, X., Lu, S., & Zhang, J. (2022). Learning disentangled representation implicitly via transformer for occluded person re-identification. *IEEE Transactions on Multimedia*.
- Jin, H., Lai, S., & Qian, X. (2021). Occlusion-sensitive person re-identification via attribute-based shift attention. *IEEE Transactions on Circuits and Systems for Video Technology*, 32(4), 2170–2185.
- Kalayeh, M. M., Basaran, E., Gökmen, M., Kamasak, M. E., & Shah, M. (2018). Human semantic parsing for person re-identification. In *Proceedings of the IEEE conference on computer vision and pattern recognition* (pp. 1062–1071).
- Kanazawa, A., Black, M. J., Jacobs, D. W., & Malik, J. (2018). End-to-end recovery of human shape and pose. In *Proceedings of the IEEE conference on computer vision and pattern recognition* (pp. 7122–7131).
- Khan, S., Naseer, M., Hayat, M., Zamir, S. W., Khan, F. S., & Shah, M. (2022). Transformers in vision: A survey. *ACM computing surveys (CSUR)*, 54(10s), 1–41.
- Kim, J. & Yoo, C. D. (2017). Deep partial person re-identification via attention model. In *2017 IEEE International Conference on Image Processing (ICIP)* (pp. 3425–3429).: IEEE.
- Kim, M., Cho, M., Lee, H., Cho, S., & Lee, S. (2022). Occluded person re-identification via relational adaptive feature correction learning. In *ICASSP 2022-2022 IEEE International Conference on Acoustics, Speech and Signal Processing (ICASSP)* (pp. 2719–2723).: IEEE.
- Kiran, M., Praveen, R. G., Nguyen-Meidine, L. T., Belharbi, S., Blais-Morin, L.-A., & Granger, E. (2021). Holistic guidance for occluded person re-identification. *arXiv preprint arXiv:2104.06524*.
- Lavi, B., Ullah, I., Fatan, M., & Rocha, A. (2020). Survey on reliable deep learning-based person re-identification models: Are we there yet? *arXiv preprint arXiv:2005.00355*.
- Leng, Q., Ye, M., & Tian, Q. (2019). A survey of open-world person re-identification. *IEEE Transactions on Circuits and Systems for Video Technology*, 30(4), 1092–1108.
- Li, W., Zhao, R., Xiao, T., & Wang, X. (2014). Deepreid: Deep filter pairing neural network for person re-identification. In *Proceedings of the IEEE conference on computer vision and pattern recognition* (pp. 152–159).
- Li, W., Zhu, X., & Gong, S. (2018). Harmonious attention network for person re-identification. In *Proceedings of the IEEE conference on computer vision and pattern recognition* (pp. 2285–2294).
- Li, Y., Jiang, X., & Hwang, J.-N. (2020). Effective person re-identification by self-attention model guided feature learning. *Knowledge-Based Systems*, 187, 104832.
- Li, Y., Liu, L., Zhu, L., & Zhang, H. (2021). Person re-identification based on multi-scale feature learning. *Knowledge-Based Systems*, 228, 107281.
- Li, Y.-J., Chen, Y.-C., Lin, Y.-Y., Du, X., & Wang, Y.-C. F. (2019). Recover and identify: A generative dual model for cross-resolution person re-identification. In *Proceedings of the IEEE/CVF international conference on computer vision* (pp. 8090–8099).
- Liang, X., Gong, K., Shen, X., & Lin, L. (2018). Look into person: Joint body parsing & pose estimation network and a new benchmark. *IEEE transactions on pattern analysis and machine intelligence*, 41(4), 871–885.
- Lin, C.-S. & Wang, Y.-C. F. (2021). Self-supervised bodymap-to-appearance co-attention for partial person re-identification. In *2021 IEEE International Conference on Image Processing (ICIP)* (pp. 2299–2303).: IEEE.
- Lin, T.-Y., Maire, M., Belongie, S., Hays, J., Perona, P., Ramanan, D., Dollár, P., & Zitnick, C. L. (2014). Microsoft coco: Common objects in

- context. In *Computer Vision–ECCV 2014: 13th European Conference, Zurich, Switzerland, September 6–12, 2014, Proceedings, Part V 13* (pp. 740–755): Springer.
- Liu, H., Feng, J., Jie, Z., Jayashree, K., Zhao, B., Qi, M., Jiang, J., & Yan, S. (2017). Neural person search machines. In *Proceedings of the IEEE International Conference on Computer Vision* (pp. 493–501).
- Liu, J., Zha, Z.-J., Hong, R., Wang, M., & Zhang, Y. (2019). Deep adversarial graph attention convolution network for text-based person search. In *Proceedings of the 27th ACM International Conference on Multimedia* (pp. 665–673).
- Liu, Q., Teng, Q., Chen, H., Li, B., & Qing, L. (2022). Dual adaptive alignment and partitioning network for visible and infrared cross-modality person re-identification. *Applied Intelligence*, 52(1), 547–563.
- Liu, Z., Lin, Y., Cao, Y., Hu, H., Wei, Y., Zhang, Z., Lin, S., & Guo, B. (2021). Swin transformer: Hierarchical vision transformer using shifted windows. In *Proceedings of the IEEE/CVF international conference on computer vision* (pp. 10012–10022).
- Loper, M., Mahmood, N., Romero, J., Pons-Moll, G., & Black, M. J. (2015). Smpl: A skinned multi-person linear model. *ACM transactions on graphics (TOG)*, 34(6), 1–16.
- Luo, H., Jiang, W., Gu, Y., Liu, F., Liao, X., Lai, S., & Gu, J. (2019). A strong baseline and batch normneuralization neck for deep person reidentification. *arXiv preprint arXiv:1906.08332*.
- Ma, Z., Zhao, Y., & Li, J. (2021). Pose-guided inter-and intra-part relational transformer for occluded person re-identification. In *Proceedings of the 29th ACM International Conference on Multimedia* (pp. 1487–1496).
- Mao, S., Zhang, S., & Yang, M. (2019). Resolution-invariant person re-identification. *arXiv preprint arXiv:1906.09748*.
- Martinel, N., Das, A., Micheloni, C., & Roy-Chowdhury, A. K. (2016). Temporal model adaptation for person re-identification. In *Computer Vision–ECCV 2016: 14th European Conference, Amsterdam, The Netherlands, October 11–14, 2016, Proceedings, Part IV 14* (pp. 858–877): Springer.
- Miao, J., Wu, Y., Liu, P., Ding, Y., & Yang, Y. (2019). Pose-guided feature alignment for occluded person re-identification. In *Proceedings of the IEEE/CVF international conference on computer vision* (pp. 542–551).
- Miao, J., Wu, Y., & Yang, Y. (2021). Identifying visible parts via pose estimation for occluded person re-identification. *IEEE transactions on neural networks and learning systems*, 33(9), 4624–4634.
- Ming, Z., Zhu, M., Wang, X., Zhu, J., Cheng, J., Gao, C., Yang, Y., & Wei, X. (2022). Deep learning-based person re-identification methods: A survey and outlook of recent works. *Image and Vision Computing*, 119, 104394.
- Nagaraju, G., Raju, G. S. R., Ko, Y. H., & Yu, J. S. (2016). Hierarchical ni-co layered double hydroxide nanosheets entrapped on conductive textile fibers: a cost-effective and flexible electrode for high-performance pseudocapacitors. *Nanoscale*, 8(2), 812–825.
- Nguyen, D. T., Hong, H. G., Kim, K. W., & Park, K. R. (2017). Person recognition system based on a combination of body images from visible light and thermal cameras. *Sensors*, 17(3), 605.
- Ning, X., Gong, K., Li, W., & Zhang, L. (2021). Jwsaa: joint weak saliency and attention aware for person re-identification. *Neurocomputing*, 453, 801–811.
- Ning, X., Gong, K., Li, W., Zhang, L., Bai, X., & Tian, S. (2020a). Feature refinement and filter network for person re-identification. *IEEE Transactions on Circuits and Systems for Video Technology*, 31(9), 3391–3402.
- Ning, X., Nan, F., Xu, S., Yu, L., & Zhang, L. (2020b). Multi-view frontal face image generation: a survey. *Concurrency and Computation: Practice and Experience*, (pp. e6147).
- Park, H., Lee, S., Lee, J., & Ham, B. (2021). Learning by aligning: Visible-infrared person re-identification using cross-modal correspondences. In *Proceedings of the IEEE/CVF international conference on computer vision* (pp. 12046–12055).
- Peng, Y., Hou, S., Cao, C., Liu, X., Huang, Y., & He, Z. (2022). Deep learning-based occluded person re-identification: A survey. *arXiv preprint arXiv:2207.14452*.
- Qi, C. R., Su, H., Mo, K., & Guibas, L. J. (2017). Pointnet: Deep learning on point sets for 3d classification and segmentation. In *Proceedings of the IEEE conference on computer vision and pattern recognition* (pp. 652–660).
- Quispe, R., & Pedrini, H. (2019). Improved person re-identification based on saliency and semantic parsing with deep neural network models. *Image and Vision Computing*, 92, 103809.
- Ren, X., Zhang, D., & Bao, X. (2020). Semantic-guided shared feature alignment for occluded person re-identification. In *Asian Conference on Machine Learning* (pp. 17–32): PMLR.
- Ristani, E., Solera, F., Zou, R., Cucchiara, R., & Tomasi, C. (2016). Performance measures and a data set for multi-target, multi-camera tracking. In *Computer Vision–ECCV 2016 Workshops: Amsterdam, The Netherlands, October 8–10 and 15–16, 2016, Proceedings, Part II* (pp. 17–35): Springer.
- Sarfraz, M. S., Schumann, A., Eberle, A., & Stiefelhagen, R. (2018). A pose-sensitive embedding for person re-identification with expanded cross neighborhood re-ranking. In *Proceedings of the IEEE conference on computer vision and pattern recognition* (pp. 420–429).
- Sekhar, S. C., Nagaraju, G., & Yu, J. S. (2017). Conductive silver nanowires-fenced carbon cloth fibers-supported layered double hydroxide nanosheets as a flexible and binder-free electrode for high-performance asymmetric supercapacitors. *Nano Energy*, 36, 58–67.
- Shamshad, F., Khan, S., Zamir, S. W., Khan, M. H., Hayat, M., Khan, F. S., & Fu, H. (2023). Transformers in medical imaging: A survey. *Medical Image Analysis*, (pp. 102802).
- Su, C., Li, J., Zhang, S., Xing, J., Gao, W., & Tian, Q. (2017). Pose-driven deep convolutional model for person re-identification. In *Proceedings of the IEEE international conference on computer vision* (pp. 3960–3969).
- Sun, K., Xiao, B., Liu, D., & Wang, J. (2019a). Deep high-resolution representation learning for human pose estimation. In *Proceedings of the IEEE/CVF conference on computer vision and pattern recognition* (pp. 5693–5703).
- Sun, X., & Zheng, L. (2019). Dissecting person re-identification from the viewpoint of viewpoint. In *Proceedings of the IEEE/CVF conference on computer vision and pattern recognition* (pp. 608–617).
- Sun, Y., Xu, Q., Li, Y., Zhang, C., Li, Y., Wang, S., & Sun, J. (2019b). Perceive where to focus: Learning visibility-aware part-level features for partial person re-identification. In *Proceedings of the IEEE/CVF conference on computer vision and pattern recognition* (pp. 393–402).
- Sun, Y., Zheng, L., Yang, Y., Tian, Q., & Wang, S. (2018). Beyond part models: Person retrieval with refined part pooling (and a strong convolutional baseline). In *Proceedings of the European conference on computer vision (ECCV)* (pp. 480–496).
- Szegedy, C., Vanhoucke, V., Ioffe, S., Shlens, J., & Wojna, Z. (2016). Rethinking the inception architecture for computer vision. In *Proceedings of the IEEE conference on computer vision and pattern recognition* (pp. 2818–2826).
- Tan, H., Liu, X., Bian, Y., Wang, H., & Yin, B. (2021). Incomplete descriptor mining with elastic loss for person re-identification. *IEEE Transactions on Circuits and Systems for Video Technology*, 32(1), 160–171.
- Tan, H., Liu, X., Yin, B., & Li, X. (2022a). Mhsa-net: Multihead self-attention network for occluded person re-identification. *IEEE Transactions on Neural Networks and Learning Systems*.
- Tan, L., Dai, P., Ji, R., & Wu, Y. (2022b). Dynamic prototype mask for occluded person re-identification. In *Proceedings of the 30th ACM International Conference on Multimedia* (pp. 531–540).
- Tirkolaee, E. B., Goli, A., & Weber, G.-W. (2020). Fuzzy mathematical programming and self-adaptive artificial fish swarm algorithm for just-in-time energy-aware flow shop scheduling problem with outsourcing option. *IEEE transactions on fuzzy systems*, 28(11), 2772–2783.
- Tutsoy, O., Barkana, D. E., & Tugal, H. (2018). Design of a completely model free adaptive control in the presence of parametric, non-parametric uncertainties and random control signal delay. *ISA transactions*, 76, 67–77.

- Tutsoy, O. & Tanrikulu, M. Y. (2022). Priority and age specific vaccination algorithm for the pandemic diseases: a comprehensive parametric prediction model. *BMC Medical Informatics and Decision Making*, 22(1), 4.
- Wang, C., Ning, X., Sun, L., Zhang, L., Li, W., & Bai, X. (2022a). Learning discriminative features by covering local geometric space for point cloud analysis. *IEEE Transactions on Geoscience and Remote Sensing*, 60, 1–15.
- Wang, C., Wang, C., Li, W., & Wang, H. (2021a). A brief survey on rgb-d semantic segmentation using deep learning. *Displays*, 70, 102080.
- Wang, G., Yang, S., Liu, H., Wang, Z., Yang, Y., Wang, S., Yu, G., Zhou, E., & Sun, J. (2020a). High-order information matters: Learning relation and topology for occluded person re-identification. In *Proceedings of the IEEE/CVF conference on computer vision and pattern recognition* (pp. 6449–6458).
- Wang, G., Zhang, T., Cheng, J., Liu, S., Yang, Y., & Hou, Z. (2019a). Rgb-infrared cross-modality person re-identification via joint pixel and feature alignment. In *Proceedings of the IEEE/CVF International Conference on Computer Vision* (pp. 3623–3632).
- Wang, J., Tan, S., Zhen, X., Xu, S., Zheng, F., He, Z., & Shao, L. (2021b). Deep 3d human pose estimation: A review. *Computer Vision and Image Understanding*, 210, 103225.
- Wang, P., Ding, C., Shao, Z., Hong, Z., Zhang, S., & Tao, D. (2022b). Quality-aware part models for occluded person re-identification. *IEEE Transactions on Multimedia*.
- Wang, Q., Huang, H., Zhong, Y., Min, W., Han, Q., Xu, D., & Xu, C. (2022c). Swin transformer based on two-fold loss and background adaptation re-ranking for person re-identification. *Electronics*, 11(13), 1941.
- Wang, Q., Qi, M., Jin, K., & Jiang, J. (2020b). Deep-shallow occlusion parallelism network for person re-identification. In *Journal of Physics: Conference Series*, volume 1518 (pp. 012026).: IOP Publishing.
- Wang, T., Liu, H., Song, P., Guo, T., & Shi, W. (2022d). Pose-guided feature disentangling for occluded person re-identification based on transformer. In *Proceedings of the AAAI Conference on Artificial Intelligence*, volume 36 (pp. 2540–2549).
- Wang, X., Li, C., & Ma, X. (2022e). Cross-modal local shortest path and global enhancement for visible-thermal person re-identification. *arXiv preprint arXiv:2206.04401*.
- Wang, Y., Liang, X., & Liao, S. (2022f). Cloning outfits from real-world images to 3d characters for generalizable person re-identification. In *Proceedings of the IEEE/CVF Conference on Computer Vision and Pattern Recognition* (pp. 4900–4909).
- Wang, Z., Wang, Z., Wu, Y., Wang, J., & Satoh, S. (2019b). Beyond intra-modality discrepancy: A comprehensive survey of heterogeneous person re-identification. *arXiv preprint arXiv:1905.10048*, 4.
- Wang, Z., Wang, Z., Zheng, Y., Chuang, Y.-Y., & Satoh, S. (2019c). Learning to reduce dual-level discrepancy for infrared-visible person re-identification. In *Proceedings of the IEEE/CVF conference on computer vision and pattern recognition* (pp. 618–626).
- Wang, Z., Zhu, F., Tang, S., Zhao, R., He, L., & Song, J. (2022g). Feature erasing and diffusion network for occluded person re-identification. In *Proceedings of the IEEE/CVF Conference on Computer Vision and Pattern Recognition* (pp. 4754–4763).
- Wen, X., Feng, X., Li, P., & Chen, W. (2022). Cross-modality collaborative learning identified pedestrian. *The Visual Computer*, (pp. 1–16).
- Wu, A., Zheng, W.-S., & Lai, J.-H. (2017a). Robust depth-based person re-identification. *IEEE Transactions on Image Processing*, 26(6), 2588–2603.
- Wu, A., Zheng, W.-S., Yu, H.-X., Gong, S., & Lai, J. (2017b). Rgb-infrared cross-modality person re-identification. In *Proceedings of the IEEE international conference on computer vision* (pp. 5380–5389).
- Wu, Y., Lin, Y., Dong, X., Yan, Y., Ouyang, W., & Yang, Y. (2018). Exploit the unknown gradually: One-shot video-based person re-identification by stepwise learning. In *Proceedings of the IEEE conference on computer vision and pattern recognition* (pp. 5177–5186).
- Xie, Y., Tian, J., & Zhu, X. X. (2020). Linking points with labels in 3d: A review of point cloud semantic segmentation. *IEEE Geoscience and remote sensing magazine*, 8(4), 38–59.
- Xu, B., He, L., Liang, J., & Sun, Z. (2022). Learning feature recovery transformer for occluded person re-identification. *IEEE Transactions on Image Processing*, 31, 4651–4662.
- Xu, J., Zhao, R., Zhu, F., Wang, H., & Ouyang, W. (2018). Attention-aware compositional network for person re-identification. In *Proceedings of the IEEE conference on computer vision and pattern recognition* (pp. 2119–2128).
- Xu, Y., Zhao, L., & Qin, F. (2021). Dual attention-based method for occluded person re-identification. *Knowledge-Based Systems*, 212, 106554.
- Yaghoubi, E., Kumar, A., & Proença, H. (2021). Sss-pr: A short survey of surveys in person re-identification. *Pattern Recognition Letters*, 143, 50–57.
- Yan, C., Pang, G., Jiao, J., Bai, X., Feng, X., & Shen, C. (2021). Occluded person re-identification with single-scale global representations. In *Proceedings of the IEEE/CVF International Conference on Computer Vision* (pp. 11875–11884).
- Yang, J., Zhang, C., Tang, Y., & Li, Z. (2022). Pafm: pose-drive attention fusion mechanism for occluded person re-identification. *Neural Computing and Applications*, 34(10), 8241–8252.
- Yang, J., Zhang, J., Yu, F., Jiang, X., Zhang, M., Sun, X., Chen, Y.-C., & Zheng, W.-S. (2021). Learning to know where to see: A visibility-aware approach for occluded person re-identification. In *Proceedings of the IEEE/CVF international conference on computer vision* (pp. 11885–11894).
- Yang, W., Yan, Y., Chen, S., Zhang, X., & Wang, H. (2020). Multi-scale generative adversarial network for person reidentification under occlusion. *Journal of Software*, 31(7), 1943–1958.
- Ye, M., Chen, C., Shen, J., & Shao, L. (2021a). Dynamic tri-level relation mining with attentive graph for visible infrared re-identification. *IEEE Transactions on Information Forensics and Security*, 17, 386–398.
- Ye, M., Shen, J., J. Crandall, D., Shao, L., & Luo, J. (2020). Dynamic dual-attentive aggregation learning for visible-infrared person re-identification. In *Computer Vision—ECCV 2020: 16th European Conference, Glasgow, UK, August 23–28, 2020, Proceedings, Part XVII 16* (pp. 229–247).: Springer.
- Ye, M., Shen, J., Lin, G., Xiang, T., Shao, L., & Hoi, S. C. (2021b). Deep learning for person re-identification: A survey and outlook. *IEEE transactions on pattern analysis and machine intelligence*, 44(6), 2872–2893.
- Zhai, Y., Han, X., Ma, W., Gou, X., & Xiao, G. (2021). Pgmanet: Pose-guided mixed attention network for occluded person re-identification. In *2021 International Joint Conference on Neural Networks (IJCNN)* (pp. 1–8).: IEEE.
- Zhang, C., Liu, H., Guo, W., & Ye, M. (2021). Multi-scale cascading network with compact feature learning for rgb-infrared person re-identification. In *2020 25th International Conference on Pattern Recognition (ICPR)* (pp. 8679–8686).: IEEE.
- Zhang, G., Chen, C., Chen, Y., Zhang, H., & Zheng, Y. (2022a). Fine-grained-based multi-feature fusion for occluded person re-identification. *Journal of Visual Communication and Image Representation*, 87, 103581.
- Zhang, L., Guo, H., Zhu, K., Qiao, H., Huang, G., Zhang, S., Zhang, H., Sun, J., & Wang, J. (2022b). Hybrid modality metric learning for visible-infrared person re-identification. *ACM Transactions on Multimedia Computing, Communications, and Applications (TOMM)*, 18(1s), 1–15.
- Zhang, Q., Dang, K., Lai, J.-H., Feng, Z., & Xie, X. (2022c). Modeling 3d layout for group re-identification. In *Proceedings of the IEEE/CVF Conference on Computer Vision and Pattern Recognition* (pp. 7512–7520).
- Zhang, X., Yan, Y., Xue, J.-H., Hua, Y., & Wang, H. (2020). Semantic-aware occlusion-robust network for occluded person re-identification. *IEEE Transactions on Circuits and Systems for Video Technology*, 31(7), 2764–2778.
- Zhang, Y. & Lu, H. (2018). Deep cross-modal projection learning for image-text matching. In *Proceedings of the European conference on computer vision (ECCV)* (pp. 686–701).

- Zhang, Z., Lan, C., Zeng, W., & Chen, Z. (2019). Densely semantically aligned person re-identification. In *Proceedings of the IEEE/CVF conference on computer vision and pattern recognition* (pp. 667–676).
- Zhao, C., Lv, X., Dou, S., Zhang, S., Wu, J., & Wang, L. (2021). Incremental generative occlusion adversarial suppression network for person reid. *IEEE Transactions on Image Processing*, 30, 4212–4224.
- Zhao, R., Ouyang, W., & Wang, X. (2013). Unsupervised salience learning for person re-identification. In *Proceedings of the IEEE conference on computer vision and pattern recognition* (pp. 3586–3593).
- Zhao, S., Gao, C., Zhang, J., Cheng, H., Han, C., Jiang, X., Guo, X., Zheng, W.-S., Sang, N., & Sun, X. (2020). Do not disturb me: Person re-identification under the interference of other pedestrians. In *Computer Vision–ECCV 2020: 16th European Conference, Glasgow, UK, August 23–28, 2020, Proceedings, Part VI 16* (pp. 647–663): Springer.
- Zhao, Y., Zhu, S., Wang, D., & Liang, Z. (2022). Short range correlation transformer for occluded person re-identification. *Neural computing and applications*, 34(20), 17633–17645.
- Zheng, K., Lan, C., Zeng, W., Liu, J., Zhang, Z., & Zha, Z.-J. (2021). Pose-guided feature learning with knowledge distillation for occluded person re-identification. In *Proceedings of the 29th ACM International Conference on Multimedia* (pp. 4537–4545).
- Zheng, L., Shen, L., Tian, L., Wang, S., Wang, J., & Tian, Q. (2015a). Scalable person re-identification: A benchmark. In *Proceedings of the IEEE international conference on computer vision* (pp. 1116–1124).
- Zheng, L., Yang, Y., & Hauptmann, A. G. (2016). Person re-identification: Past, present and future. *arXiv preprint arXiv:1610.02984*.
- Zheng, M., Karanam, S., Wu, Z., & Radke, R. J. (2019). Re-identification with consistent attentive siamese networks. In *Proceedings of the IEEE/CVF conference on computer vision and pattern recognition* (pp. 5735–5744).
- Zheng, W.-S., Gong, S., & Xiang, T. (2011). Person re-identification by probabilistic relative distance comparison. In *CVPR 2011* (pp. 649–656): IEEE.
- Zheng, W.-S., Li, X., Xiang, T., Liao, S., Lai, J., & Gong, S. (2015b). Partial person re-identification. In *Proceedings of the IEEE international conference on computer vision* (pp. 4678–4686).
- Zheng, Z., Wang, X., Zheng, N., & Yang, Y. (2022). Parameter-efficient person re-identification in the 3d space. *IEEE Transactions on Neural Networks and Learning Systems*.
- Zheng, Z., Zheng, L., & Yang, Y. (2017). Unlabeled samples generated by gan improve the person re-identification baseline in vitro. In *Proceedings of the IEEE international conference on computer vision* (pp. 3754–3762).
- Zhong, Y., Wang, X., & Zhang, S. (2020a). Robust partial matching for person search in the wild. In *Proceedings of the IEEE/CVF conference on computer vision and pattern recognition* (pp. 6827–6835).
- Zhong, Z., Zheng, L., Kang, G., Li, S., & Yang, Y. (2020b). Random erasing data augmentation. In *Proceedings of the AAAI conference on artificial intelligence*, volume 34 (pp. 13001–13008).
- Zhou, K., Yang, Y., Cavallaro, A., & Xiang, T. (2019). Omni-scale feature learning for person re-identification. In *Proceedings of the IEEE/CVF international conference on computer vision* (pp. 3702–3712).
- Zhou, M., Liu, H., Lv, Z., Hong, W., & Chen, X. (2022). Motion-aware transformer for occluded person re-identification. *arXiv preprint arXiv:2202.04243*.
- Zhou, Q., Zhong, B., Lan, X., Sun, G., Zhang, Y., Zhang, B., & Ji, R. (2020a). Fine-grained spatial alignment model for person re-identification with focal triplet loss. *IEEE Transactions on Image Processing*, 29, 7578–7589.
- Zhou, S., Wu, J., Zhang, F., & Sehdev, P. (2020b). Depth occlusion perception feature analysis for person re-identification. *Pattern Recognition Letters*, 138, 617–623.
- Zhu, K., Guo, H., Liu, Z., Tang, M., & Wang, J. (2020). Identity-guided human semantic parsing for person re-identification. In *Computer Vision–ECCV 2020: 16th European Conference, Glasgow, UK, August 23–28, 2020, Proceedings, Part III 16* (pp. 346–363): Springer.
- Zhu, X., Zheng, M., Chen, X., Zhang, X., Yuan, C., & Zhang, F. (2022). Information disentanglement based cross-modal representation learning for visible-infrared person re-identification. *Multimedia Tools and Applications*, (pp. 1–27).
- Zhuo, J., Chen, Z., Lai, J., & Wang, G. (2018). Occluded person re-identification. In *2018 IEEE International Conference on Multimedia and Expo (ICME)* (pp. 1–6): IEEE.
- Zhuo, J., Lai, J., & Chen, P. (2019). A novel teacher-student learning framework for occluded person re-identification. *arXiv preprint arXiv:1907.03253*.